Energy dependence of cross sections for double-electron capture in 48–132-keV C^{6+}+He collisions

J.-Y. Chesnel, H. Merabet, X. Husson, F. Frémont and D. Lecler
Laboratoire de Spectroscopie Atomique, Institut des Sciences de la Matière et du Rayonnement, 6 Boulevard Maréchal Juin, F-14050 Caen Cedex, France

H. Jouin and C. Harel
Centre de Physique Théorique et de Modélisation de Bordeaux, URA 1537 du CNRS, Laboratoire des Collisions Atomiques, Université Bordeaux I, 351 Cours de la Libération, F-33405 Talence Cedex, France

N. Stolterfoht
Hahn-Meitner Institut GmbH, Bereich Festkörperphysik, Glienickerstrasse 100, D-14109 Berlin, Germany
(Received 20 June 1995)

We report on the projectile energy dependence of the cross sections for producing the configurations $2lnl'$ ($n \geq 3$) by double-electron capture in C^{6+}+He collisions. The present measurements and calculations, which extend previous work performed on the 90-keV C^{6+}+He system, give evidence for dynamic electron-correlation effects in double-capture mechanisms. A significant dependence on the collision energy is found for the cross sections associated with the configurations $2lnl'$ ($n \geq 5$). Moreover, anisotropies of the angular distributions of Auger electrons originating from the configurations $2l3l'$ are observed at 48 and 132 keV. The capture cross sections for producing some of the terms $2l3l'\ ^1L$ are shown to depend on the collision energy. The cross sections for production of the magnetic substates $M_L=0$ associated with the configurations $2l3l'$ are found to be the same for both energies of 48 and 132 keV.

PACS number(s): 32.80.Hd, 34.50.−s

I. INTRODUCTION

The study of two-electron capture into slow, multiply charged ions interacting with few-electron atoms is currently of considerable interest [1–5]. During the past few years, experimental work has been devoted to determining the cross sections for producing configurations $2lnl'$ ($n \geq 3$) in 60 to 90-keV C^{6+}+He collisions [6–9]. The mechanisms for the production of these excited final states have been the object of several theoretical studies and extensive discussions [6–14]. Dynamic electron-correlation effects have been invoked in order to explain the production of autoionizing states $2lnl'$ with nonequivalent electrons [6]. These correlation effects can be discussed by means of the potential-curve diagram in Fig. 1 which illustrates resonance conditions at different potential-curve crossings [8].

Considering first the case of the *near*-equivalent configuration $2l3l'$ (summed over l and l'), resonance conditions for a first monoelectronic transition are created by the crossing (near 5 a.u.) between the potential curves attributed to the entrance C^{6+}+He channel and the single-capture channel $C^{5+}(3l)+He^{+}$. At smaller internuclear distances (< 2 a.u.), a further crossing allows a second single-electron transition from the intermediate $C^{5+}(3l)+He^{+}$ state to the final double-capture state $C^{4+}(2l3l')+He^{2+}$. Hence, a two-step mechanism involving two monoelectronic processes caused by the nucleus-electron interaction may create the configuration $2l3l'$ of quasiequivalent electrons. However, a dielectronic process, denoted correlated double capture (CDC), may also populate this configuration. These alternative paths have been treated in theoretical studies. Chen *et al.* [11] performed calculations within the framework of the independent-particle model. They suggested that the monoelectronic processes are responsible for the $2l3l'$ production, whereas Harel, Jouin, and Pons [12], taking into account the electron-electron interaction, concluded that the configuration $2l3l'$ may be produced by dielectronic processes. Hence, the mechanisms for populating configurations of near-equivalent electrons ($2l3l'$) are still under debate, since controversial models [11–14] are invoked for their understanding.

However, for the case of configurations of *nonequivalent* electrons (e.g., $2l6l'$) the uncorrelated processes are unlikely, since monoelectronic transitions can be ruled out [6]. In this case, the CDC process is expected to occur as the incident C^{6+}+He channel crosses the double-electron-capture $C^{4+}(2l6l')+He^{2+}$ channel near 4 a.u. Furthermore, correlated two-step mechanisms may also lead to the production of the configuration $2l6l'$. A first monoelectronic transition, creating the $C^{5+}(3l)+He^{+}$ state, is followed by a correlated transfer (projectile) excitation (CTE) processes involving a two-electron transition into the double-capture state $2l6l'$. Likewise, a first correlated transfer (target) excitation (CTE) involves a two-electron transfer, producing the $C^{5+}(2l)+He^{+}(\tilde{n}\tilde{l})$ state (with, e.g., $\tilde{n}=4$). The final $C^{4+}(2l6l')+He^{2+}$ state is then populated by the transfer of the helium electron in the state $\tilde{n}$ to the Rydberg level $6l'$ of carbon, producing also the configuration $2l6l'$. It is noted that both CDC and CTE processes, created by the electron-electron interaction, are examples of the dielectronic processes of *autoexcitation* [10].

In the present work, we investigate the dependence of the

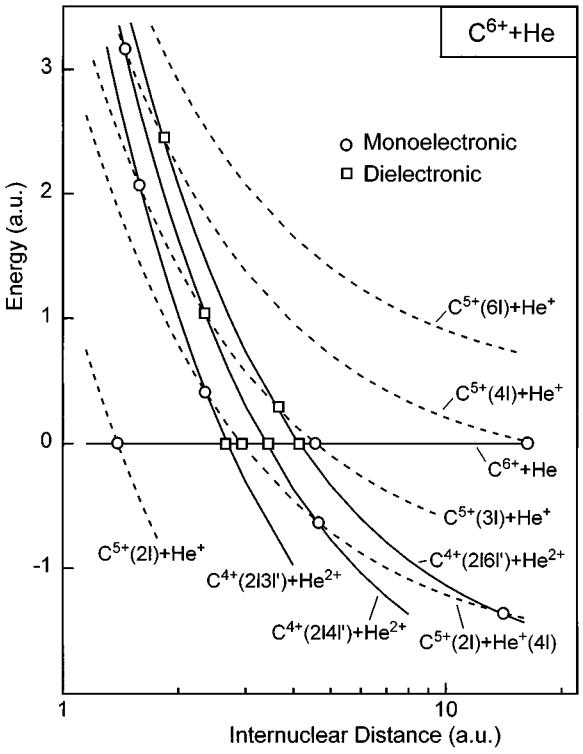

FIG. 1. Diagram for approximate potential curves of the $C^{6+}+He$ system. A limited number of potential curves relevant for the production of configurations $2lnl'$ $(n=3-6)$ is shown. Dashed lines and solid lines correspond to single and double capture, respectively.

double-electron-capture process on the collision energy in order to gain additional insights into the mechanisms populating the final configurations $2lnl'$. We measured energy spectra of autoionization electrons arising from collisions of bare C^{6+} ions on He atoms at incident energies of 48 and 132 keV (i.e., at the projectile velocities of 0.39 and 0.64 a.u., respectively). In particular, we studied angular distributions of Auger electrons ejected from the decay of the series $2lnl'$ $(n\geqslant 3)$. The results yield the corresponding double-capture cross sections. Theoretical calculations of total cross sections were performed and are compared with the experimental data. Furthermore, high-resolution measurements allowed the study of the capture process producing the terms $2l3l'\ ^1L$ and their magnetic substate $M_L=0$.

II. EXPERIMENTAL METHOD AND DATA ANALYSIS

Highly charged ions were produced by the 14-GHz electron cyclotron resonance (ECR) ion source at the test bench of the Grand Accélérateur National d'Ions Lourds in Caen (France). The C^{6+} ions were accelerated and, after mass analysis, were transported to a vacuum-scattering chamber with a background pressure of around 10^{-7} mbar. For the production of the ion beam, ^{13}C isotopes were used in order to avoid beam contamination with other ions of charge-to-mass ratio equal to $\frac{1}{2}$. The beam was collimated to a diam. of 2 mm, adjusted with two beam steerers and slightly focused with an Einzel lens. An ion current of about 25 nA was directed into a helium-gas target created by an effusive gas jet. The average target pressure was estimated to be $\approx 10^{-4}$ mbar. This pressure was kept low to reduce multiple collisions for the incident C^{6+} ions.

To perform the experiment, the electron-spectroscopy apparatus [15] from the Hahn-Meitner Institut in Berlin was used. The Auger electrons that were ejected from the target region were energy analyzed using a tandem 0° electron spectrometer as well as a single-stage spectrometer, which consists of 90° parallel-plate analyzers, and detected by a channeltron electron multiplier. The entrance analyzer of the tandem spectrometer was used to deflect the Auger electrons out of the beam and to suppress background electrons. The exit analyzer determined the electron energy with the resolution of 5% full width at half maximum. By decelerating the electrons to 20 eV in the intermediate region between the analyzers (high-resolution mode), a constant energy resolution of 1 eV was achieved. The data were accumulated and further processed by a personal computer. This processing took into account the variation of the channeltron efficiency as a function of the electron energy and the Doppler shift of the emitted electrons. More details about the experimental setup and method were given previously [15].

To evaluate absolute cross sections, the measurements of low-resolution Auger spectra were used to normalize the spectra measured with high resolution [8]. To determine single differential cross sections $d\sigma^a_{2,n}/d\Omega$ for Auger-electron emission attributed to the configurations $2lnl'$ (summed over l and l'), the high-resolution Auger spectra were numerically integrated with respect to electron energy. Total cross sections $\sigma^a_{2,n}$ for Auger emission were evaluated by integration of $d\sigma^a_{2,n}/d\Omega$ over the electron-emission angles (θ). Since radiative transitions are in competition with K-Auger autoionization processes, cross sections $\sigma_{2,n}$ for production of doubly excited states $2lnl'$ were obtained using the relation

$$\sigma_{2,n}=\frac{\sigma^a_{2,n}}{a_{2,n}}, \tag{1}$$

where $a_{2,n}$ are the corresponding mean Auger yields determined previously [6]. The absolute uncertainties for the obtained results are 30% and the relative uncertainties with respect to a variation of the emission angle are 20%. These uncertainties increase for the series members $2l6l'$ and $2l7l'$.

To analyze the angular distribution of Auger-electron emission, calculated curves were fitted to the experimental data (Fig. 2). Within the framework of the LS-coupling scheme the angular distribution of an individual state with angular momentum L, decaying to a final S state, is given by [16]

$$\frac{d\sigma^a_{2lnl'\ ^1L}}{d\Omega}(\theta)=\sum_{M_L=-L}^{L}\sigma^a_{2lnl'\ ^1L,M_L}\left|Y_L^{M_L}(\theta)\right|^2, \tag{2}$$

where $Y_L^{M_L}(\theta)$ are spherical harmonics and $\sigma^a_{2lnl'\ ^1L,M_L}$ are total cross sections for Auger emission following the decay of the magnetic substate $|2lnl'\ ^1L;M_L\rangle$. The quantization axis is chosen to be parallel to the internuclear axis between the collision partners. Since the square of $Y_L^{M_L}(\theta)$ occurs

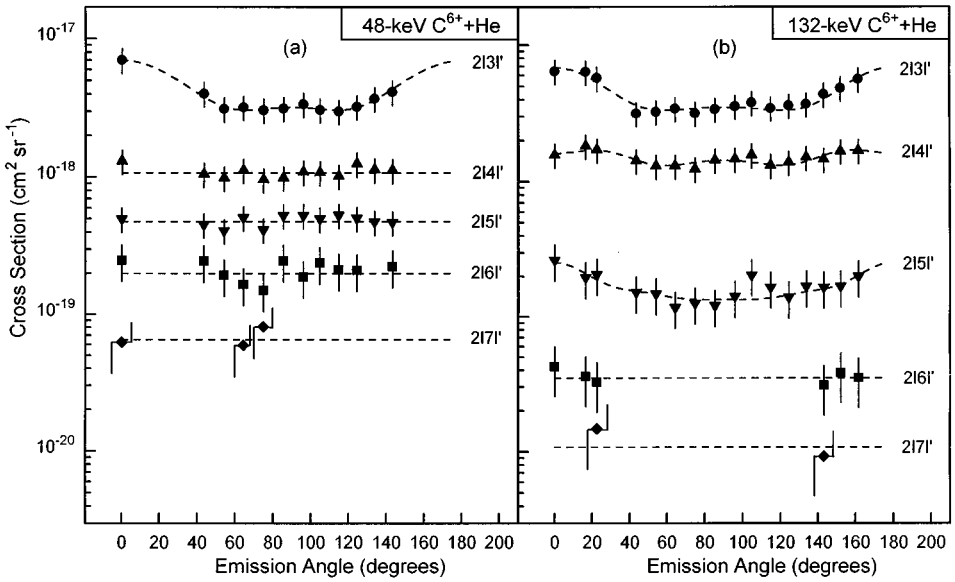

FIG. 2. Single differential cross sections for Auger-electron emission associated with the configurations $2lnl'$ ($n=3$–7). The dashed lines represent fits to the experimental data (see the text). In (a) and (b) collision energies of 48 and 132 keV are used, respectively.

in Eq. (2) the theoretical angular distributions of the Auger electrons are sums of expressions $a_{2m}\cos^{2m}\theta$ ($m=0,\ldots,L_{\max}$, with $L_{\max}=n$). Thus, it follows that the angular distributions are symmetric with respect to $\theta=90°$. However, it should be emphasized that the electric field of the remaining target nucleus He^{2+} produces Stark effects, which may create deviations from this $\theta=90°$ symmetry [17]. However, such effects could not be detected within the present experimental uncertainties.

As shown in the next section, the knowledge of the probability $Q(2l3l';M_L=0)$ for population of magnetic substates $M_L=0$ when referred to $2l3l'$ was needed to obtain more information on the double-capture event populating the configuration $2l3l'$. The probability $Q(2l3l';M_L=0)$ is given by

$$Q(2l3l';M_L=0)=\frac{1}{\sigma_{2,3}}\left(\sum_L \frac{\sigma^a_{2l3l'\ ^1L,M_L=0}}{a_{2l3l'\ ^1L}}\right), \qquad (3)$$

where $a_{2l3l'\ ^1L}$ are the individual Auger yields calculated by Van der Hart and Hansen [18] and $\sigma_{2,3}$ is the total cross section for the production of the configuration $2l3l'$ [determined by Eq. (1) and given in Table I]. Taking into account Eq. (2), the cross sections $\sigma^a_{2l3l'\ ^1L,M_L=0}$ were obtained as

$$\sigma^a_{2l3l'\ ^1L,M_L=0}=\frac{4\pi}{(2L+1)}\frac{d\sigma^a_{2l3l'^1L}}{d\Omega}(\theta=0°), \qquad (4)$$

where $|Y^0_L(\theta=0°)|^2=(2L+1)/4\pi$ was used. The differential cross sections $d\sigma^a_{2l3l'\ ^1L}/d\Omega$ ($\theta=0°$) were determined by measuring high-resolution spectra at 0° (Fig. 3). The Auger energies associated with the terms $2l3l'\ ^1L$ were calculated previously [6]. These theoretical results were used to deconvolute the experimental data. Since asymmetric line shapes due to postcollisional effects [19] were estimated to be small, we fitted the spectra with Gaussian curves. Examples for the fit curves are seen in Fig. 3. From these fits, differential cross sections $d\sigma^a_{2l3l'\ ^1L}/d\Omega(\theta=0°)$ were evaluated by integrating each Gaussian peak.

III. RESULTS AND DISCUSSIONS

A. Angular distribution for the configurations $2lnl'$

Figure 2 shows the angular distribution of K-Auger electrons ejected after double-electron-capture in 48 and 132-

TABLE I. Total cross sections for producing the doubly excited configurations $2lnl'$ ($n\geqslant 3$) in 48-, 90-, and 132-keV C^{6+}+He collisions. The data for 90 keV were measured previously by Frémont and collaborators [9].

	$\sigma_{2,n}$ (10^{-18} cm^2)				
Collision energy (keV)	$2l3l'$	$2l4l'$	$2l5l'$	$2l6l'$	$2l7l'$
48	68.0±13.6	25.8±5.2	17.5±3.5	9.2±1.8	5.0±1.5
90	64.6±12.9	29.3±5.9	9.6±2.9	6.6±2.0	3.6±1.1
132	72.0±14.4	34.0±6.8	5.7±1.7	1.6±0.5	0.7±0.2

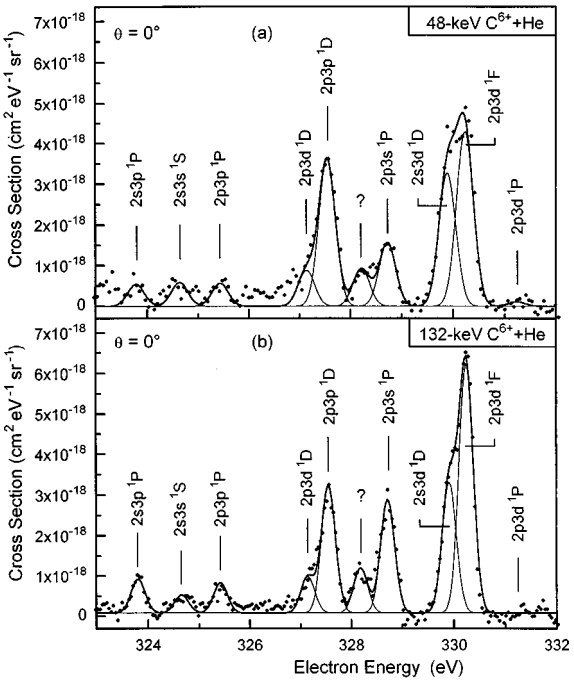

FIG. 3. High-resolution 0° spectra yielding double differential cross sections associated with the production of the configurations $2l3l'$ in C^{6+}+He collisions. Each peak, representing a Gaussian curve, corresponds to the Auger decay of the state $2l3l'\ ^1L$. In (a) and (b) incident energies of respectively 48 and 132 keV are used.

keV C^{6+}+He collisions. It is seen that the electron emission from the decay of the configuration $2l3l'$ is anisotropic for both studied collision energies. Similar results have been obtained at the intermediate collision energy of 90 keV by Frémont *et al.* [9], who observed an anisotropy for both the configurations $2l3l'$ and $2l4l'$. In the present measurements, an anisotropic Auger emission for the configurations $2l4l'$ and $2l5l'$ can also be invoked at the impact energy of 132 keV, whereas the corresponding cross sections for 48 keV were found to be isotropic within the experimental uncertainties. Furthermore, taking into account experimental error bars, an isotropy can be considered for the configurations $2l6l'$ and $2l7l'$ in the energy range from 48 to 132 keV.

The observed anisotropies are due to a selectivity in the population of a given M_L magnetic substate, which gives rise to an alignment propensity for the states produced by the double-capture processes. Since the function $|Y_L^{M_L}(\theta)|^2$ vanishes at $\theta=0°$ for $M_L\neq 0$, the Auger-electron emission at 0° provides a measure for the $M_L=0$ cross section of the state $2lnl'\ ^1L$. From the observation that the differential $\theta=0°$ cross section is larger than the corresponding ones for $\theta\neq 0°$, it follows that the probability for populating the magnetic substate $M_L=0$ of the series $2lnl'$ is generally higher than that for populating the components $M_L\neq 0$. This $M_L=0$ predominance implies an alignment along the beam direction of the states $2lnl'$, as shown by Frémont *et al.* [9] for the case of the *near*-equivalent electron configuration $2l3l'$ produced in the 90-keV C^{6+}+He collision. The finding of alignment effects in *double*-electron-transfer processes extends the picture of propensity rules [20,21]. These rules have been verified from the orientation effects observed for *single*-electron capture in 1.5–12 keV $B^{3+}(1s^2)$+He collisions [22] as well as for *single*-electron transfer from initial-circular atomic states in keV H^++Na($3p$) collisions [23].

TABLE II. Differential cross sections $d\sigma^a_{2l3l'\ ^1L}/d\Omega$ ($\theta=0°$) for the Auger emission from the doubly excited $2l3l'\ ^1L$ states. Each value of $d\sigma^a_{2l3l'\ ^1L}/d\Omega$ ($\theta=0°$) is the average of the results obtained by fitting several analogous high-resolution spectra, and the corresponding uncertainty is the standard deviation of these results. The labels (a) and (b) correspond to the collision energies of 48 and 132 keV, respectively.

	$d\sigma^a_{2l3l'\ ^1L}/d\Omega(\theta=0°)(10^{-18}$ cm^2 sr^{-1})	
Terms $2l3l'\ ^1L$	(a)	(b)
$2p3d\ ^1F$	1.75±0.26	2.11±0.32
$2s3d\ ^1D$	1.33±0.20	1.11±0.17
$2p3p\ ^1D$	1.47±0.29	1.08±0.22
$2p3d\ ^1D$	0.36±0.11	0.31±0.09
$2s3p\ ^1P$	0.22±0.11	0.29±0.15
$2p3p\ ^1P$	0.20±0.10	0.26±0.13
$2p3s\ ^1P$	0.64±0.13	0.96±0.19
$2p3d\ ^1P$	0.05±0.03	⩽0.01
$2s3s\ ^1S$	0.24±0.12	0.15±0.07

To illustrate the alignment effects we consider the processes involved in the double-capture event producing the *near*-equivalent electron configurations $2l3l'$. Although the dielectronic process CDC can be invoked in the production of $2l3l'$, a significant contribution of uncorrelated processes to the production of this state is expected. The nucleus-electron interaction is the principal cause for such monoelectronic processes. As transfers due to the nucleus-electron interaction are directed towards the projectile nucleus, the internuclear direction provides a symmetry axis. Moreover, resonance conditions for the corresponding monoelectronic transfers as well as for the CDC transition are created at internuclear distances (Fig. 1), that are larger than the dimension of the projectile orbitals $2l$ and $3l'$ [24]. Consequently, the dominant component of the initial and final states of the transient quasimolecule is Σ ($M_L=0$), where quantization is along the internuclear axis that corresponds asymptotically to the beam direction. Hence, the double-electron-capture processes producing the configuration $2l3l'$ are expected to involve an electronic charge cloud aligned along the beam axis.

To gain additional insights into the anisotropic angular distribution for the configuration of *near*-equivalent electrons $2l3l'$, high-resolution 0° spectra, including the terms $2l3l'\ ^1L$ were measured (Fig. 3 and Table II). The probability $Q(2l3l';M_L=0)$ was evaluated to be equal to 0.32 for both impact energies of 48 and 132 keV. The same value was obtained by Frémont and co-workers [9] at the intermediate energy of 90 keV, where cross sections for producing $M_L=0$ substates were shown to be dominant. An alignment of the configuration $2l3l'$ along the beam axis is observed for both 48 and 132-keV C^{6+}+He collision systems. This alignment is rather independent on the projectile velocity in the energy range from 48 to 132 keV. We note that the

present results should not be generalized. Different from the present results, Prior and collaborators [25] have recently shown, for the double capture by H-like ions C^{5+} and B^{4+} from He atoms, that the production of the M_L states depends sensitively on the collision energy.

For the higher values of the principal quantum number n of the Rydberg electron, Fig. 2 indicates that the angular distributions of the configurations $2lnl'$ are isotropic. As pointed out before [8] in accordance with Harel, Jouin, and Pons [12], dielectronic processes (such as CDC and CTE) are responsible for the production of the configurations of *non-equivalent* electrons $2lnl'$ with $n \geqslant 5$. It is noted that the nucleus-electron interaction is represented by a one-body Hamiltonian that cannot be responsible for a two-body mechanism, such as a dielectronic process. Hence, although a significant attraction of the electrons by the multiply charged projectile occurs during the double-capture event, the electron-electron interaction plays the major role in producing the states $2lnl'$ $(n \geqslant 5)$. One He electron is transferred towards the C^{6+} nucleus, while the other one is autoexcited, via the dielectronic interaction, to occupy the Rydberg level (as $6l$). Orbitals with spherical-like symmetry are therefore created, since the autoexcited electron is pushed up in any direction. Hence, the observed isotropies associated with the configurations $2lnl'$ of high n quantum number are consistent with the finding that the dielectronic interaction is the driving force for producing these states.

B. Total cross sections for the production of the configurations $2lnl'$

The total cross sections $\sigma_{2,n}$ for the production of the configurations $2lnl'$ $(n \geqslant 3)$ were evaluated by using Eq. (1) (see Fig. 4 and Table I). The cross sections attributed to the configurations $2l3l'$ and $2l4l'$ are found to be independent of the projectile velocity in the energy range from 48 to 132 keV. However, the production of the states $2lnl'$ $(n \geqslant 5)$ appears to depend significantly on the collision energy. In particular, these cross sections are found to decrease strongly for 132-keV impact, i.e., the highest energy studied here. One may therefore conclude that in slow C^{6+}+He collisions the mechanisms producing the near-equivalent electron configurations ($2l3l'$ and to a certain extend $2l4l'$) and the nonequivalent electron configurations $(n \gtrsim 5)$ are different.

Particular attention was devoted to the correlated processes such as CDC and CTE, which are likely to be responsible for the production of the nonequivalent electron configurations. Taking into account the dielectronic interaction, the total cross sections for producing the configurations $2lnl'$ $(3 \leqslant n \leqslant 6)$ were calculated. The framework of the theoretical method is the same as that described in Refs. [12,26]. In a straight-line impact-parameter treatment, the total electronic wave function is expanded onto a set of configurations built with product of one-electron diatomic-molecular orbitals (OEDM), which are exact solutions of a one-electron two-center Hamiltonian. The electronic momentum transfer is taken into account through the same two-electron common translation factor as in [12] and [27]. In the range of impact velocities investigated here, we have checked that the results are completely insensitive to the

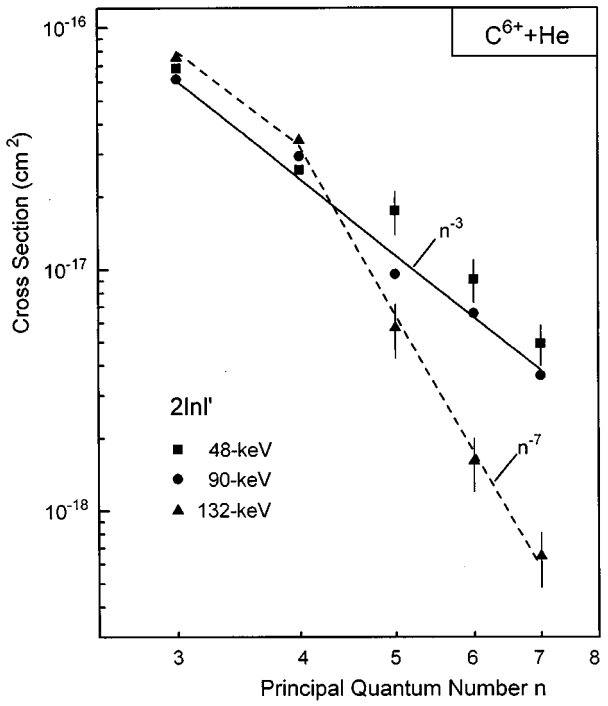

FIG. 4. Total cross sections for the production of the configurations $2lnl'$ $(n \geqslant 3)$ in 48-, 90-, and 132-keV C^{6+}+He collisions. The solid line represents a n^{-3} curve normalized to fit the experimental data for 90 keV [9]. The dashed line represents a fit to the experimental cross sections obtained for 132-keV C^{6+}+He collisions. At 132 keV, the cross sections attributed to the configurations $2lnl'$ with $n \geqslant 5$ are found to depend on the principal quantum number n approximately as n^{-7}.

choice of the parameter α appearing in the switching function $g_\alpha(\mu)$ (see [12] and [27]). Furthermore, as we are interested here in calculating the global population of some members of the $2lnl'$ series, in the molecular expansion we have only introduced a few configurations for each corresponding double-capture channel. Our choice is based on the dynamical quasiselection rules of the OEDM orbitals discussed previously [28]. In the present calculations we have used a basis set of 15 dielectronic configurations, which allows one to represent the $n=3$ and 4 single-capture channels (the $n=3$ capture channel being dominantly populated by single-electron capture in C^{6+}+He collisions; see [12]) and also the dielectronic excited states $3l3l'$ and $2lnl'$ with $n=3$–6. The introduction of the above expansion in the Schrödinger equation leads to a set of coupled equations that is numerically integrated using a vectorized version of the PAMPA code [29]. The results are shown in Table III and are compared with the experimental data in Fig. 5.

There is a rather good agreement between the *ab initio* calculations and the experimental results. Nevertheless, differences of about a factor of 2 between calculation and experimental values occur, particularly at the highest projectile velocity investigated here (0.64 a.u.). However, the most significant comparison between theory and experiment concerns the velocity dependence of the cross sections. The cross sections for populating the configurations $2lnl'$ with $n \geqslant 3$ are theoretically found to be rather constant with respect to the collision velocity. This is in complete agreement with the

TABLE III. Theoretical total cross sections for producing the configurations $2lnl'$ ($n \geqslant 3$) in $C^{6+}+He$ collisions. The projectile velocities of 0.39, 0.53, and 0.64 a.u. are respectively associated with the collision energies of 48, 90, and 132 keV, the energies experimentally studied.

Projectile velocity (a.u.)	Projectile energy (keV)	$\sigma_{2,n}$ (10^{-18} cm^2)			
		$2l3l'$	$2l4l'$	$2l5l'$	$2l6l'$
0.21	15	33	16	9	7
0.30	29	35	21	13	6
0.39	48	53	22	13	4
0.53	90	40	27	13	6
0.64	132	32	16	10	3

experiment for the case of the near-equivalent electron configurations $2l3l'$ and $2l4l'$. On the contrary, for the nonequivalent electron states $2l5l'$ and $2l6l'$ the theory disagrees with the experiment, since a strong variation with projectile velocity is experimentally found for the cross sections associated with these states.

It should be pointed out here that the population of the terms $2lnl'\,{}^1L$ associated with a give quantum number n depends on the collision energy. Consequently, each average Auger yield $a_{2,n}$ corresponding to the configuration $2lnl'$ may vary with respect to the projectile velocity. Nevertheless, the mean Auger yields determined previously [6] in the case of the 60-keV $C^{6+}+He$ collisions were utilized to evaluate cross sections for double-electron capture in 48-, 90-, and 132-keV $C^{6+}+He$ collisions. However, the observed differences of about a factor of 2 between the calculated and the experimental cross sections cannot be explained by the fact that the velocity dependence of the average Auger yields was not taken into account [6]. Moreover, it should be noted that, in order to avoid numerical problems produced by the strong variation of the radial coupling between the $4f\sigma$ and $3d\sigma$ OEDM orbitals around the internuclear distance $R=7$ a.u., we have used a diabatization procedure along the lines described in [30]. This procedure makes the calculations more elaborate and, thus, limits the basis sets [in opposition with the cases of N^{7+}, O^{8+}, and $Ne^{8+}+He(1s^2)$ collisions previously studied by means of the same theoretical treatment [26,27]]. Hence, uncertainties of about 20% can be attributed to the calculated cross sections associated with the near-equivalent electron configurations $2l3l'$ and $2l4l'$, while uncertainties as large as 50% can be invoked for the calculation results in the case of the low populated diffuse configurations $2l5l'$ and $2l6l'$.

The experimental results are consistent with the feature that dielectronic processes of autoexcitation are responsible for the population of nonequivalent electron configurations. This is in complete agreement with the results of test calculations as reported in [31]. We only summarize here the conclusions of these test calculations: We have performed two test calculations in which we cancel successively (i) the couplings between the entry channel and the double-electron-capture (DEC) channels or (ii) the couplings between the single-electron-capture (SEC) channel into $n=3$ and the DEC channels. In (i), we obtain a much smaller value for the cross section corresponding to the configuration $2l3l'$ (in comparison with the full calculation), whereas the cross sections for capture into $2lnl'$ ($n \geqslant 4$) remain unchanged. In (ii), the inverse result is obtained. So, direct transitions of both electrons are principally responsible for the production of the configuration $2l3l'$ (CDC process), whereas the states $2lnl'$ ($n \geqslant 4$) are dominantly produced from two-step transitions through the SEC channel into $n=3$. In this latter case,

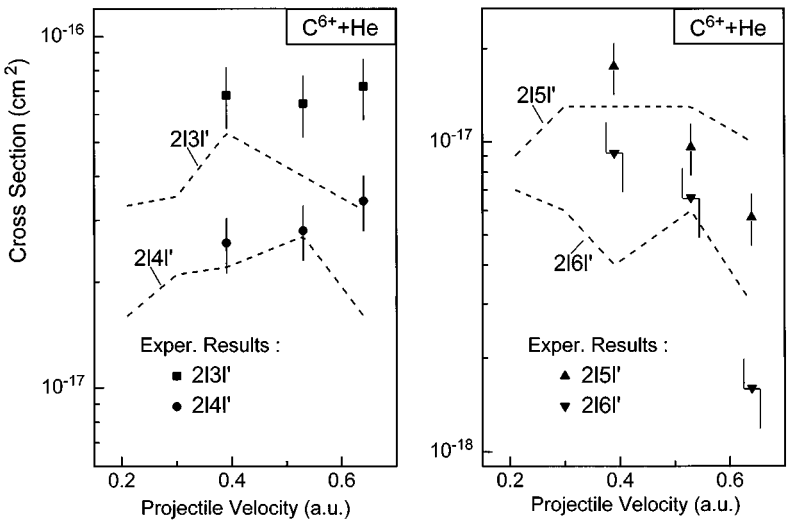

FIG. 5. Total cross sections for the production of the configurations $2lnl'$ ($3 \leqslant n \leqslant 6$) in $C^{6+}+He$ collisions. The theoretical results (dashed line) are shown in comparison with the experimental data (solid symbols). The projectile velocities of 0.39, 0.53, and 0.64 a.u. are respectively associated with the collision energies of 48, 90, and 132 keV, the energies experimentally studied.

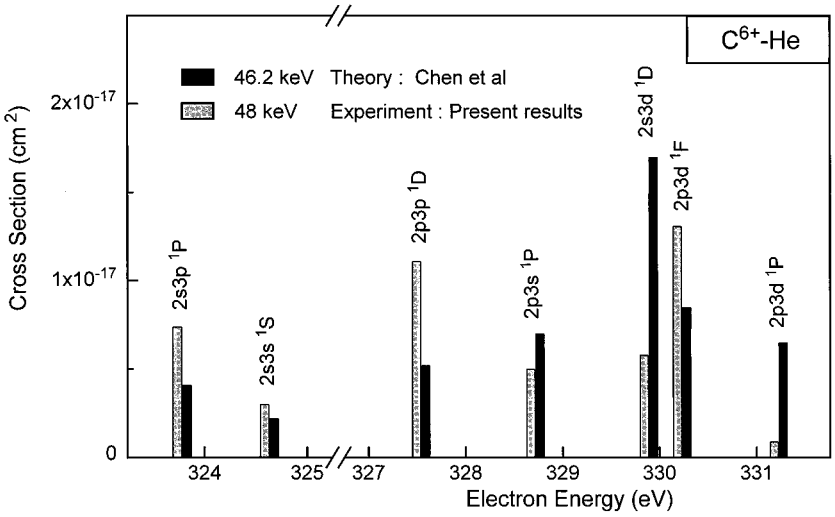

FIG. 6. Total cross sections for the production of the terms $2l3l'\ ^1L$ in comparison with theoretical calculations performed by Chen and co-workers [11].

the state of the first captured electron is changed when the second one is captured (CTE process). Undoubtedly, the electron-electron interaction plays a dominant role in both types of processes, leading to the formation of the doubly excited states $2lnl'$ in C^{6+}+He collisions at low-impact energies.

C. Cross sections for producing the terms $2l3l'\ ^1L$

To study the energy dependence of the cross sections for populating the substates $2l3l'\ ^1L$, high-resolution measurements were performed. The experimental data of the differential cross sections $d\sigma^a_{2l3l'\ ^1L}/d\Omega(\theta=0°)$ for Auger-electron emission from the doubly excited states $2l3l'\ ^1L$ are shown in Table II. From these results, it follows that the production of the terms $2l3l'\ ^1L$ depends rather weakly on the collision energy. Actually, the observed variations of the corresponding cross sections are in the same order as the experimental uncertainties. The most significant variation of cross sections is noted for the term $2p3s\ ^1P$ and also for $2p3d\ ^1F$, $2s3d\ ^1D$, and $2p3p\ ^1D$, which include relatively high angular momenta. It is reasonable to invoke some specific effects in the production of the high angular momenta.

The summed cross section, which takes into account the production of the terms $2l3l'\ ^1D$ and $2p3d\ ^1F$, was found to be rather independent of the collision energy. Hence, the production of the term $2p3d\ ^1F$ may occur in competition with the production of the terms $2l3l'\ ^1D$, since the population of $2p3d\ ^1F$ increases with collision energy, whereas the populations of the terms $2l3l'\ ^1D$ decrease. Besides, a noticeable increase with respect to the projectile energy was observed for the production of the term $2p3s\ ^1P$, while the production of $2p3d\ ^1P$ was found to become negligible at 132 keV. Taking into account experimental error bars, no significant energy dependence can be observed for the other terms (Table II).

Previously, Chen and co-workers [11] have performed theoretical work to calculate the total cross sections $\sigma_{2l3l'\ ^1L}$ for producing the terms $2l3l'\ ^1L$ in the 46.2-keV C^{6+}+He collision system. The collision energy investigated by these authors is close to the present energy of 48 keV. It is therefore of considerable interest to compare our experimental data obtained at 48 keV with these previous theoretical results. To estimate total cross sections $\sigma_{2l3l'\ ^1L}$ by means of the measured differential cross sections $d\sigma^a_{2l3l'\ ^1L}/d\Omega$ $(\theta=0°)$, it is necessary to take into account the individual Auger yields $a_{2l3l'\ ^1L}$ as well as the probabilities $Q(2l3l'\ ^1L;M_L=0)$ for producing the magnetic substate $M_L=0$ of the terms $2l3l'\ ^1L$. Since the production of the terms $2l3l'\ ^1L$ was not found to depend sensitively on the impact energy within the experimental uncertainties (Table II), it is reasonable to assume that the probabilities $Q(2l3l'\ ^1L;M_L=0)$ are constant in the energy range from 48 to 132 keV. Hence, the values of $Q(2l3l'\ ^1L;M_L=0)$ determinated by Frémont *et al.* [9] for the 90-keV C^{6+}+He system were utilized to estimate the cross sections $\sigma_{2l3l'\ ^1L}$ at 48 keV. The results of the estimate and the comparison with the theoretical results of Chen and co-workers [11] are shown in Fig. 6.

The theoretical and the experimental data disagree, particularly for the terms $2l3l'\ ^1D$ as well as for $2p3d\ ^1P$. However, there is a surprisingly good agreement for the particular case of the summed cross sections, including the productions of the high angular-momentum terms $2l3l'\ ^1D$ and $2p3d\ ^1F$. Good agreements occur also for the $L=0$ term $2s3s\ ^1S$ and the term $2p3s\ ^1P$. Moreover, the sum of the experimental cross sections for producing the terms $2l3l'\ ^1L$ agrees well with the theoretical data.

It should be pointed out that Chen *et al.* [11] have performed their cross-section calculations within the framework of the independent-electron approximation. As illustrated in the potential-curve diagram (Fig. 1) and shown by our test calculations, a significant contribution of the correlated CDC process for the production of the configuration $2l3l'$ is expected. Hence, to increase the agreement between theory and experiment, further calculations, including the electron-electron interaction are needed. It should also be recalled that the present experimental cross sections involve uncertainties, since simple Gaussian curves were used to fit the measured spectra and, furthermore, each $Q(2l3l'\ ^1L;M_L=0)$ were assumed to be constant with respect to the collision energy. Consequently, to determine more exactly the cross sections $\sigma_{2l3l'\ ^1L}$, further angular distribution measurements of the corresponding Auger electrons are required.

IV. CONCLUSION

In this work we report on the collision energy dependence of cross sections for the production of the configurations $2lnl'$ $(n \geqslant 3)$ in double-electron-capture collisions of C^{6+} with He. The cross sections for creating the configurations of near-equivalent electrons ($n=3$ and to a certain extent $n=4$) are shown to be rather constant in the studied energy range. Furthermore, the angular distributions of Auger electrons originating from these near-equivalent electron configurations are found to be anisotropic. On the contrary, a significant variation with the projectile energy is experimentally found for the cross sections associated with the configurations $2lnl'$ $(n \geqslant 5)$ of nonequivalent electrons. At the collision energies of 48 and 90 keV, the cross sections for populating the configurations $2lnl'$ $(n \geqslant 5)$ are shown to depend on the quantum number n approximately as n^{-3}, while they are found to follow rather a n^{-7} dependence at 132 keV. In previous work, a n^{-3} dependence has been found for the cross sections attributed to the configurations $2lnl'$. The present studies show that this dependence should not be generalized.

The present experimental and calculation results show that the dielectronic process CTE contributes dominantly to the production of nonequivalent electron states, while the population of near-equivalent electron states involves uncorrelated two-electron transfers as well as a dielectronic (CDC) process. High-resolution measurements were performed for individual terms attributed to the configuration $2l3l'$. A significant impact-velocity dependence of the capture cross sections is found for some terms $2l3l'\ ^1L$. Nevertheless the same propensity rule, favoring the $M_L=0$ population, is observed in the studied energy range. Further work is suggested to progress in the understanding of charge-transfer dynamics and orientation propensity of the autoionizing states produced in slow multiply charged ion-atom collisions.

ACKNOWLEDGMENTS

We are grateful to Alain Lepoutre for providing the data-acquisition computer program. We are much indebted to the staff of the ECR source at the Grand Accélérateur National d'Ions Lourds (GANIL) for their generous assistance. Illuminating discussions with Dominique Hennecart and Alain Bordenave-Montesquieu are gratefully acknowledged. This work was supported by the European Collaboration Research Program PROCOPE. The calculations reported here were supported by the Centre National Universitaire Sud de Calcul (Montpellier, France) and by the Conseil Régional d'Aquitaine.

[1] A. Bordenave-Montesquieu, P. Benoit-Cattin, A. Gleizes, A. I. Marrakachi, S. Dousson, and D. Hitz, J. Phys. B **17**, L223 (1984).
[2] N. Stolterfoht, C. C. Havener, R. A. Phaneuf, J. K. Swensen, S. M. Shafroth, and F. W. Meyer, Phys. Rev. Lett. **57**, 74 (1986).
[3] P. Roncin, M. Barat, and H. Laurent, Europhys. Lett. **2**, 371 (1986).
[4] M. Mack, J. H. Nijland, P. v. d. Straten, A. Niehaus and R. Morgenstern, Phys. Rev. A **39**, 3846 (1989).
[5] F. Fremont, H. Merabet, J.-Y. Chesnel, X. Husson, A. Lepoutre, D. Lecler, and N. Stolterfoht, Phys. Rev. A **50**, 3117 (1994).
[6] N. Stolterfoht, K. Sommer, J. K. Swenson, C. C. Havener, and F. W. Meyer, Phys. Rev. A **42**, 5396 (1990).
[7] H. A. Sakaue, Y. Kanai, K. Ohta, M. Kushina, T. Inaba, S. Ohtani, K. Wakiya, H. Suzuki, T. Takayanagi, T. Kambara, A. Danjo, M. Yoshino, and Y. Awaya, J. Phys. B **23**, L401 (1990).
[8] F. Frémont, K. Sommer, D. Lecler, S. Hicham, X. Husson, and N. Stolterfoht, Phys. Rev. A **46**, 222 (1992).
[9] F. Frémont, K. Sommer, S. Hicham, P. Boduch, D. Lecler, and N. Stolterfoht, Nucl. Instrum. Methods B **79**, 3 (1993).
[10] N. Stolterfoht, Phys. Scr. **42**, 192 (1990).
[11] Z. Chen, R. Singal, and C. D. Lin, J. Phys. B **24**, 4215 (1991); Z. Chen and C. D. Lin, *ibid.* **24**, 4231 (1991).
[12] C. Harel, H. Jouin, and B. Pons, J. Phys. B **24**, L425 (1991).
[13] N. Stolterfoht, Phys. Scr. **T51**, 39 (1994).
[14] M. Barat and P. Roncin, J. Phys. B **25**, 2205 (1992).
[15] N. Stolterfoht, Z. Phys. **248**, 81 (1971); **248**, 92 (1971); A. Itoh, T. Schneider, G. Schiwietz, Z. Roller, H. Platten, G. Nolte, D. Schneider, and N. Stolterfoht, J. Phys. B **16**, 3965 (1983).
[16] B. Cleff and W. Mehlhorn, J. Phys. B **7**, 593 (1974).
[17] N. Stolterfoht, D. Brandt, and M. Prost, Phys. Rev. Lett. **43**, 1654 (1979).
[18] H. W. Van der Hart and J. E. Hansen, J. Phys. B **26**, 641 (1993).
[19] R. B. Barker and H. W. Berry, Phys. Rev. **151**, 14 (1966).
[20] N. Andersen and S. E. Nielsen, Z. Phys. D **5**, 309 (1987).
[21] S. E. Nielsen, J. P. Hansen, and A. Dubois, J. Phys. B **23**, 2595 (1990).
[22] P. Roncin, C. Adjouri, M. N. Gaboriaud, L. Guillemot, M. Barat, and N. Andersen, Phys. Rev. Lett. **65**, 3261 (1990).
[23] J. C. Houver, D. Dowek, C. Richter, and N. Andersen, Phys. Rev. Lett. **68**, 162 (1992).
[24] A. Messiah, *Quantum Mechanics* (North-Holland, Amsterdam, 1970), Vol. II.
[25] M. H. Prior, R. A. Holt, D. Schneider, K. L. Randall, and R. Hutton, Phys. Rev. A **48**, 1964 (1993).
[26] C. Harel and H. Jouin, Europhys. Lett. **11**, 121 (1990).
[27] C. Harel and H. Jouin, J. Phys. B **25**, 221 (1992).
[28] C. Harel and A. Salin, *Invited Papers of the Fifteenth International Conference on Physics of Electronic and Atomic Collisions, Brighton, 1988*, edited by H. B. Gilbody, W. R. Newell, F. H. Read, and A. C. H. Smith (North-Holland, Amsterdam, 1988), p. 631.
[29] A. Salin, Comput. Phys. Commun. **62**, 58 (1991).
[30] M. Terao, C. Harel, A. Salin, and R. J. Allan, Z. Phys. D **7**, 319 (1988).
[31] C. Harel, H. Jouin, and B. Pons, *Proceedings of the VIth International Conference on the Physics of Highly Charged Ions, Manhattan, Kansas, 1992*, edited by P. Richard, M. Stockli, and C. D. Lin, AIP Conf. Proc. No. 274 (AIP, New York, 1993), p. 179.